ELSEVIER

Clinical Neurophysiology 115 (2004) 227–237

www.elsevier.com/locate/clinph

A novel spatio-temporal decomposition of the EEG: derivation, validation and clinical application

Clive Jackson*, Michael Sherratt

EEG Department, Royal Free Hospital NHS Trust, Pond Street, London NW3 2QG, UK

Accepted 5 September 2003

Abstract

Objective: To obtain clinically useful graphical and numerical data on the distribution of activities in the EEG using a novel type of spatio-temporal decomposition.

Methods: The EEG is divided into 1/4 s epochs. An approximation to the spatial distribution of the locally dominant activity in each epoch is represented as a point in a spatial component space. Points representing epochs dominated by activity from the same source form a cluster. The centres of these clusters represent the global spatial component of each source. As each spatial component is identified, its corresponding temporal activity is removed from the record, allowing activity from sources with smaller amplitude to become dominant in the reduced record. Successive components are identified in the reduced record. The method was applied to 40 normal EEGs and features were identified, which were common to them all. The method was also applied to 4 separate records with different forms of focal abnormality.

Results: The method successfully separated components from the EEG representing alpha rhythm, eye artefact, electrode artefact and EEG. In 40 normal EEGs the method isolated spatial components that were common to all EEGs, and in 4 abnormal EEGs it achieved a high degree of mutual separation of alpha rhythm, focal spikes, focal theta and focal delta activities.

Conclusions: The method achieved a high degree of mutual separation of the EEG components and successfully differentiated the artefacts due to eye movement, ECG and electrode faults. The clinical implications are discussed.

Keywords: Spatio-temporal decomposition; Feature extraction; Artefact; Principal component analysis; Cluster analysis; Blind separation; Focal activity; Reconstruction

1. Introduction

The EEG can be mathematically decomposed into a set of components, each with separate spatial and temporal parts (Scherg and Von Cramon, 1985, Koles, 1991). If the decomposition is confined to describing the distribution of components across the scalp, no model of the head or its contents is required (Koles, 1998). The decomposition can be done in an infinite number of ways, producing components that are mutually orthogonal, including principal component analysis (PCA) (Lamothe and Stroink, 1991; Lagerlund, 1998), PCA with Varimax Rotation (Kaiser, 1958), common spatial pattern decomposition (Koles, 1991; Wang et al., 1999), and independent component analysis (Vigario, 1997; Kobayashi et al., 1999, 2001; Jung et al., 2000), but these methods do not separate activities into temporal waveforms that are unambiguously recognisable to the electroencephalographer. Each of these methods defines the decomposition in terms of a statistical measurement that the temporal or spatial components should satisfy, and all of these methods are 'blind', in that no knowledge of the underlying spatial or temporal components of the EEG is known.

In this report a new method of spatio-temporal decomposition is described which produces spatial components, which are not orthogonal, and rather more importantly, in temporal components that are clinically recognisable. The application of this method in the clinical setting is illustrated.

* Corresponding author. Tel.: +44-20-7830-2072; fax: +44-20-7830-2866.

E-mail address: clive.jackson@royalfree.nhs.uk (C. Jackson).

1388-2457/$30.00
doi:10.1016/j.clinph.2003.09.016

2. Methods

2.1. The new spatio-temporal decomposition technique

A 'source' is defined in this paper as being the fixed, hypothetical generator of a discrete EEG activity and its corresponding spatial activity, reflected in a scalp recording.

Two main assumptions were made: (i) that the activity from each source within the head has a constant distribution across the scalp; and (ii) that the activity from each of the sources is not correlated with the activity from other sources.

2.2. Mathematical considerations

PCA was used as the starting point for this new spatio-temporal decomposition. It results in sets of orthonormal spatial and temporal components. If an EEG reflects the activity of just one source, PCA results in only one component with non-zero amplitude. The temporal component is a normalised representation of the electrical activity emanating from the source, and the spatial component describes the normalised distribution of that activity across the channels of the EEG.

If an EEG reflects the activities of two uncorrelated sources, and low-level background noise, the PCA will generally fail to separate the main activities. Instead, the first temporal component will be a mixture of activities from the two sources, accounting for a maximal variance of the constituent activities in the EEG. The corresponding spatial component will also be a mixture, derived from the spatial distributions of the original sources. However, there may be an epoch in this EEG in which the activity from one source will dominate the activity of the other source, and the background. The result of applying the PCA to such an epoch will be similar to the single source example described above. The first principal component will provide an approximate description of the activity of interest, and its distribution. The ratio of the activity due to the first component and the total activity of the epoch is used as an indication of the accuracy of the estimate ('accuracy value').

The EEG may contain several such epochs, and the PCA can be applied separately to each, giving a collection of separate estimates of the activity and distribution of the dominant source. The spatial components will be similar to one another, as they are estimates of the distribution of activity from the same source, though the corresponding temporal components will be dissimilar.

A spatial component is an N-dimensional vector of unit length, where N is the number of channels of the EEG. A single spatial component can be represented by a single point in an N-dimensional space, the vector being the imaginary line from the origin to the point. If spatial components are normalised, points will lie on the surface of a hyper-sphere, of unit radius, centred on the origin. Experimentally derived points, that represent epochs largely dominated by one of the activities being decomposed, will tend to congregate. If these points are then averaged, their random distances from the actual position of the source should cancel out, thereby providing an improved estimate of the source position.

A cluster is defined in this paper as the site where the density of points is high relative to the background density; and the cluster centre is defined as the site of maximum density. An approximation to the density at every plotted (experimental) point was calculated by summing a weighted contribution from points within a neighbourhood, where a boundary was set arbitrarily at a threshold distance of 0.25. The contributions to the local density were weighted by distance, since the presence of nearby points automatically indicated a high density, and by their accuracy value, since points with a high accuracy value were presumed to be a better estimate of a global spatial component than points with a low accuracy value. The point with the highest weighted density value was then identified as the provisional estimate of the cluster centre.

This estimate of the cluster centre was further refined by averaging the positions of the points within the neighbourhood of this single point, each point again weighted by its accuracy value. This new estimate of the centre of the cluster of points in spatial-component space was then used as the final estimate of the global spatial component for that source of activity.

In order to facilitate analysis of activity from sources making a small contribution to the EEG, an estimate of the activity of the sources, already identified, was removed from the EEG – as each cluster was found. The PCA was applied to the epochs of this reduced EEG, and the points representing the new first spatial component from each epoch were then found, potentially revealing any clusters previously obscured. The procedure was iterated until a predetermined limit was reached, and a set of n spatial components obtained (Appendix A).

The n spatial components found by this iterative process formed an orthogonal set, confirmed by showing that the dot product between the different vectors was zero.

In order to improve the estimate of source positions in N-dimensional space, the orthogonal constraint needed to be removed; the final, step of the process was the rotation of each spatial component back into the dimensions from which it was excluded in the reduced record. The first component did not need rotation. The second component only needed rotation in the direction of the first component. The third component required rotation in the direction of the first two components, and so on.

In practice it is not possible to anticipate where epochs, dominated by same source activity, start and end, so epochs of a fixed arbitrary length were used. With a short epoch length, first, the relative levels of activity from the sources can be expected to remain constant, i.e. the EEG should be stationary during the epoch. Second, the numbers of epochs from which estimates of locally dominant

activities can be obtained are then large. Third the PCA, performed to obtain the estimate of the dominant activity in each epoch, uses the covariance between the EEG channels to calculate the eigenvectors, so the epoch length needs to be long enough for the values of covariance to be meaningful. As a compromise, an epoch length of a 1/4 s was used.

2.3. EEG acquisition

The EEG recordings were obtained using conventional protocols on a Micromed System98® or Medtronic Walter Graphtek PL Winsor® system, using 10–20 electrode placements. Filters were set at 70 Hz low pass with a time constant of 0.3 s. Signals were sampled at 256 samples per second at 12 bit digital resolution, 244 nV per bit on the Micromed system, 166 samples per second on the Walter Graphtek system. The records were later low-pass filtered at 20 Hz to attenuate any muscle activity prior to analysis. The analysis was performed on the 21 channel average reference montaged data.

The mathematical analysis was undertaken on a PC compatible computer running Windows 98® or later, using 16 bit software written in C++; it took about 1 min to analyse 1 min of a 21 channel recording.

2.4. Selection of records

A single, normal EEG recording of 20 min duration was used to develop and refine the analytical technique and was analysed in extenso. A further 40 EEGs, reported as showing 'nothing abnormal', in the departmental database of adult routine recordings, were selected for test purposes; 2-min segments were extracted from each resting record for analysis. Recordings from 4 cases with focal EEG abnormalities were analysed in extenso.

A simple K-means cluster analysis was used to determine which spatial components were common among the 40 example EEGs. We used the un-signed dot product (DP) between spatial component vectors as a measure of distance between them, as for this analysis, spatial components can be considered similar if the DP is large (1 or −1); they are very dissimilar if the value is near 0.

3. Results

3.1. In extenso analysis of the initial normal EEG

The main features in an initial 20-min EEG are summarised in the 6-s-example segment shown in Fig. 1a. They are alpha rhythm, ECG artefact, eye-related artefact, and a prominent electrode artefact, which occurred intermittently for a total of about 20 s during the entire recording on Fz. The ECG is just discernible on A2, but in other parts of the record, not shown here, in which the background is of smaller amplitude, the ECG is much more obvious.

The corresponding temporal components (Cp1–Cp21) for the same 6-s segment, based on a PCA of the entire record, are shown in Fig. 1b. The amplitudes of the temporal components reflect the relative contribution each makes to the total variance of the EEG; it is apparent that most of the variance can be attributed to the first 6 components. The first 5 components all show mixing of the alpha activity, and the eye and electrode artefacts; component Cp6 shows a clearer representation of the ECG than in the raw trace cf A2 and A1 of Fig. 1a.

The temporal components obtained using the new decomposition again scaled for their relative contribution to the EEG, are shown in Fig. 1c; most of the EEG activity can be devolved to the first 6 components. Components Cp1 and Cp2 represent the bulk of the eye artefact; the amount of 'contamination' by the alpha activity and the electrode artefact are greatly reduced, compared with the PCA components seen in Fig. 1b. Component Cp3 is a clean representation of the electrode artefact with no contaminating alpha activity, Components Cp4 and Cp5 contain the majority of the alpha activity in the record, while component Cp6 shows a clear representation of the ECG. The remaining components contribute only minimally to the EEG illustrated here.

Fig. 2 is based on the same EEG as Fig. 1. It shows just two dimensions drawn from the full N-dimensional space. The position of a point along the horizontal axis shows the relative contribution of the relevant component (see Fig. 1c) to the channel Fp2 within an epoch, and its vertical position shows the relative contribution to channel Fz. The greater the dominance of the component within an epoch, the darker the point.

The main cluster in this figure is about halfway along, and slightly above, the Fp2 axis; the size of the contribution to the remaining channels is similar to, or smaller than that to Fz-corresponding in the figure to the height above the horizontal axis. An inspection of the segments of the EEG corresponding to these epochs, confirmed that they were dominated by eye related artefact.

A second, smaller cluster of dark points lies near the top of the Fz axis. The position of these points indicates that the components make a large contribution to the Fz channel of their epochs, and a rather small contribution to Fp2. The electrode artefact appearing on channel Fz dominates these epochs. All the dimensions of the data can be dynamically displayed in random pairs on the computer monitor. This provides a visual picture of the presence or absence of clusters, which is not possible to achieve on paper.

The head-maps of the main spatial components found in the 20-min initial exemplar record are shown in Fig. 3. The maps correspond to the first 6 temporal components of Fig. 1c, which is included for comparison. The electrodes are shown as small circles, and the colour at each site shows the amplitude of the component at each; values are normalised to lie between −1 and +1 (positive values are coloured red, negative values are coloured blue).

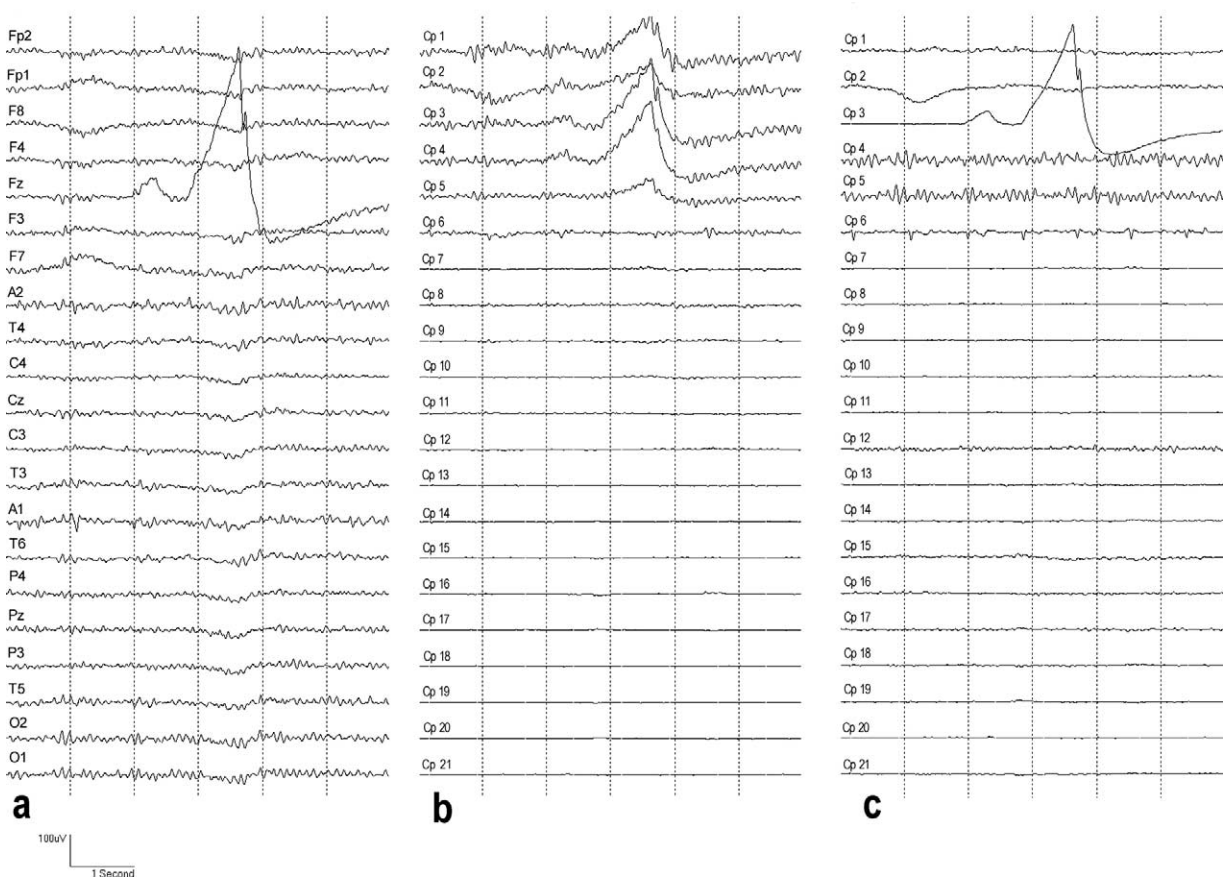

Fig. 1. (a) Six second segment of a 20 min EEG, using average reference derivations. Note the eye artefact on Fp2, Fp1, F8 and F7, the wide distribution of alpha activity, and the electrode artefact on Fz. (b) The temporal components (Cp1–Cp21) from an application of PCA to the entire record. The components are scaled according to the size of their contribution to the variance of the original EEG. The first 5 components (Cp1–Cp5) show a mixing of the main types of activity, alpha, eye and electrode artefact. (c) The temporal components produced by our method showing much improved separation of clinically recognisable activities using the new method.

The inter-electrode amplitudes are interpolated, using spherical splines (Perrin et al., 1988; Pascual-Marqui et al., 1988). Component Cp1 makes a large positive contribution on electrodes Fp2 and Fp1, while component Cp2 makes a large positive contribution in the F7 region, and a large negative contribution in the F8 region (Fig. 3b). These two components represent the majority of the eye artefact in the EEG, and the head maps indicate that this has been devolved into vertical and horizontal parts. Component Cp3 represents the electrode artefact. This component also makes small negative contributions to all other channels because of its effects on the average reference. The alpha components observed in traces Cp4 and Cp5 are shown in Figs. 3d,e. Finally the head-map corresponding to the ECG artefact seen in trace Cp6 is shown in Fig. 3f; this component makes its major contributions to electrodes A2 and A1.

3.2. Identification of variability in the 'normal' EEG

Segments from the awake EEGs of 40 adults (18 women: 22 men; mean (range) age 36 years [20–71]), were examined, to see if there was consistency of findings across subjects whose EEGs were reported as showing 'nothing abnormal'. The analysis produced a set of 840 spatial components. With K set to 5 the K-means cluster analysis produced a set of 5 clusters. When the K-means cluster analysis was repeated with K equal to 6, 7 and 8, 5 of the clusters found, in each case, were very similar to the clusters found in the original analysis. The dot product between each of the original 5 clusters, and the dot product of the corresponding new cluster found in the additional analysis exceeded 0.97, indicating that the initial 5 clusters adequately described the components common to these normal EEGs. Head-maps representing the 5 clusters are shown in Fig. 4.

The first cluster, produces a left/right symmetric head map with a maximum at Fp1 and Fp2 (Fig. 4a); this corresponds to vertical eye artefacts. Forty-one of the spatial components had a dot product of 0.9 or greater, for this cluster centre, while 47 had a dot product of 0.8 or greater. The second cluster, also produces a left/right symmetric pattern, but maximal at electrodes 01 and 02 (Fig. 4b); the corresponding temporal components consist of very smooth alpha activity. This cluster contained 24 spatial components with a dot product of 0.9 or greater for this cluster centre, and 41 with dot products of 0.8 or greater.

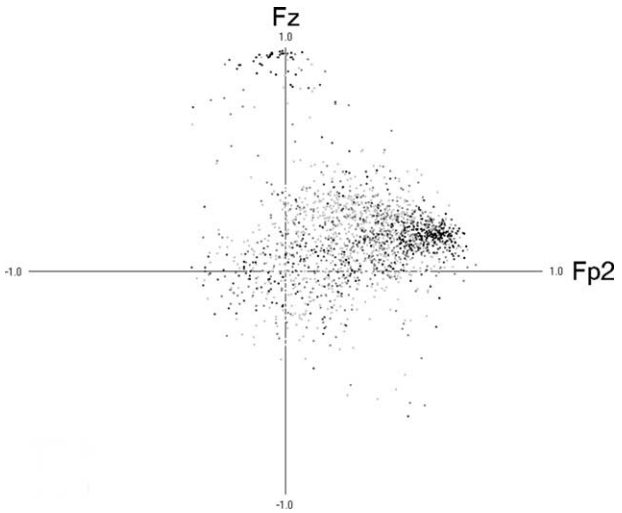

Fig. 2. Two-dimensional view of the points representing the spatial components from each 1/4 s epoch of the EEG used in Fig. 1. Points are presented in the N dimensional spatial-component space. The horizontal distance of a point from the origin represents the relative size of a component's contribution to Fp2, while the vertical distance represents the relative contribution to Fz. The more a component dominates its epoch, the darker colour of the point representing it. Two clusters are visible, the largest to the right, halfway along, and slightly above, the Fp2 axis, with a smaller cluster near the top of the Fz axis.

The head map of the third cluster has a left/right asymmetrical pattern with a positive peak near F8 and a negative peak near F7 (Fig. 4c) representing horizontal eye artefacts – e.g. left and right saccades. This cluster contained 22 spatial components with dot products of 0.9 or greater and 31 components with dot products of 0.8 or greater. The fourth cluster displayed a left/right asymmetric pattern, with a positive peak near T6 and a negative peak near T5 (Fig. 4d). The corresponding temporal components represent alpha activity, which generally is not as 'smooth' as or as large in amplitude as that in the second cluster. The numbers of points within the 0.9 and 0.8 dot product ranges were 15 and 25, respectively. The final head-map shows a peak in the Cz–Pz region (Fig. 4e). The corresponding temporal components for points near this cluster again show alpha activity; similar numbers of points were seen as in the alpha in the fourth cluster, with 13 and 24 within the 0.9 and 0.8 dot product ranges.

Most of these records contained two, or 3, significant alpha components. In most instances the main alpha spatial component showed a symmetrical posterior distribution similar to that shown in Fig. 4b. The activity was predominantly at the 01 and 02 derivations, and in phase on the left and right hand sides. A second alpha component showed an asymmetrical distribution, also in the occipital region, but 180° out of phase between the left and right sides (Fig. 3).

3.3. Analysis of abnormal EEGs

Four abnormal EEGs were analysed. The length submitted for analysis was between 10 and 20 min.

The first example, illustrated in Fig. 5, was extracted from the EEG of a 68 year-old woman with a 3-month history of daily 'absences' lasting 1–2 min. Prominent delta waves, focal between F8 and T4, small amplitude alpha activity and a large blink/eye related artefact were observed in the original EEG record (Fig. 5a). The temporal components obtained following application of the new decomposition, described in this paper, are shown in Fig. 5b. They are displayed in the order in which they were found and scaled according to their relative contribution to the variance of the EEG. Only a small number of components show any significant level of activity, leading to the conclusion that most of the activity emanates from a small number of sources. The first component represents the large eye artefact seen in the original trace in Fig. 5a, and the second component represents the abnormal focal delta activity. The remaining components contain the faster activity of the background EEG. Fig. 5c shows a reconstruction of the EEG using only component Cp2. It makes sizeable contributions to Fp2–F8, T4–T6, T4–C4 and C4–Cz, with a focal inversion near F8–T4. Fig. 5e shows a head-map representing the spatial component Cp2, with its maximum shown as a positive peak in red between F8 and T4. Fig. 5d shows a reconstruction without the second component, effectively the background EEG. It shows an almost normal background record, along with the eye artefact, suggesting that the component removed from the reconstruction represented almost all of the abnormal activity in the record.

The second example, illustrated in Fig. 6a was obtained from a 24 year-old man with a left hemiplegia due to an in utero vascular incident, and a lifelong history of focal left sided motor seizures. This record contains a normal alpha rhythm, with some eye artefacts, while F7–T3, T3–T5 and C3–T3 contain arrhythmic theta activity. The temporal components are shown in Fig. 6b. The first two components represent vertical and horizontal eye artefacts. Components Cp11 and Cp13 contain the rhythmic theta activity of interest. The remaining components represent the background activity, mainly alpha and an unrelated arrhythmic vertex theta activity in component Cp3. Fig. 6c illustrates the results of reconstructing the EEG only using components Cp11 and Cp13 while Fig. 6d shows the reconstruction using all the components, except for Cp11 and Cp13. Fig. 6e shows the head map of the spatial component corresponding to temporal component, Cp11. There is steep negative peak, as indicated by the density of the contour lines, around the T3 electrode. Fig. 6d shows an essentially normal background EEG together with arrhythmic vertex theta activity, and some vertical and horizontal eye artefact, indicating that the two removed components, Cp11 and Cp13, contained the majority of the abnormal rhythmic theta activity in the record.

The third example, illustrated in Fig. 7a, was obtained from the EEG of a 29-month old female with a 6-month history of 30-s episodes of left upper limb jerking on falling

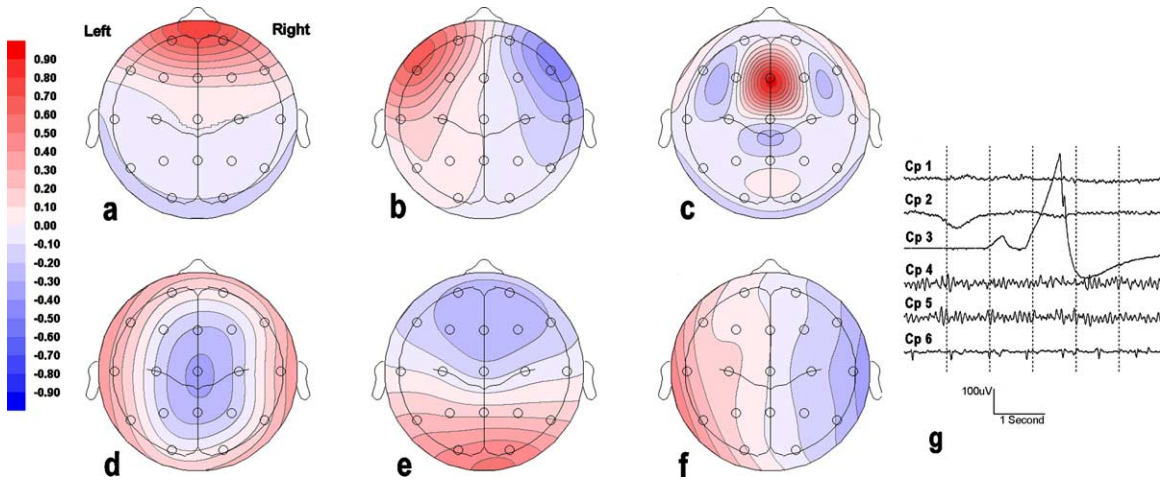

Fig. 3. Each head-map shows the spatial distribution across the scalp of the components found in the EEG used for Fig. 1: first 6 temporal components (Cp1–Cp6) are shown again in (e); (a) map of Cp1; (b) map of Cp2; (c) map of Cp3; (d) map of Cp4; (e) map of Cp5; and (f) map of Cp6.

asleep, diagnosed as benign Rolandic epilepsy. The record contains examples of singly occurring focal spikes and theta waves over an irregular background EEG. The temporal components found are shown in Fig. 7b. The nature of the general EEG background is clear from the number of components with significant activity. Most of the components are attributable to the background EEG, and components Cp3 and Cp7 are clearly attributable to eye artefact. Spike and theta wave activity are confined to only two components, Cp1 and Cp14. The head map for the main spike and theta wave component is shown in Fig. 7e; a positive peak is observed between electrodes C3 and T3, and a negative peak between the Fp1, F3 and Fz electrodes. Fig. 7c shows a reconstruction of the record using only components Cp1 and Cp14; it illustrates the distribution of the spikes in the left parieto-temporal region of the scalp. Reconstruction using the remaining components, corresponds to the background activity of the EEG (Fig. 7d).

The final example illustrated in Fig. 8a, was extracted from the EEG of a 60 year-old man with a 1 week history of focal seizures affecting the left upper and lower limb following a vascular incident leading to a left hemiparesis. It shows well-formed symmetrical alpha activity, a single eye artefact, and some recurring sharp theta waves in the left temporal region. The temporal components are illustrated in Fig. 8b. Component Cp1 represents most of the alpha activity contained in the EEG, although components Cp4, Cp5, Cp9 and Cp10 also contribute low levels of alpha activity. The eye artefact seen on channels Fp2–F4, Fp1–F3, Fp2–F8 and Fp1–F7 in Fig. 8a is represented by component Cp2 in Fig. 8b. The theta activity, seen mainly in channels Fp1–F7, F7–T3, T3–T5 and C3–T3 in Fig. 8a, is

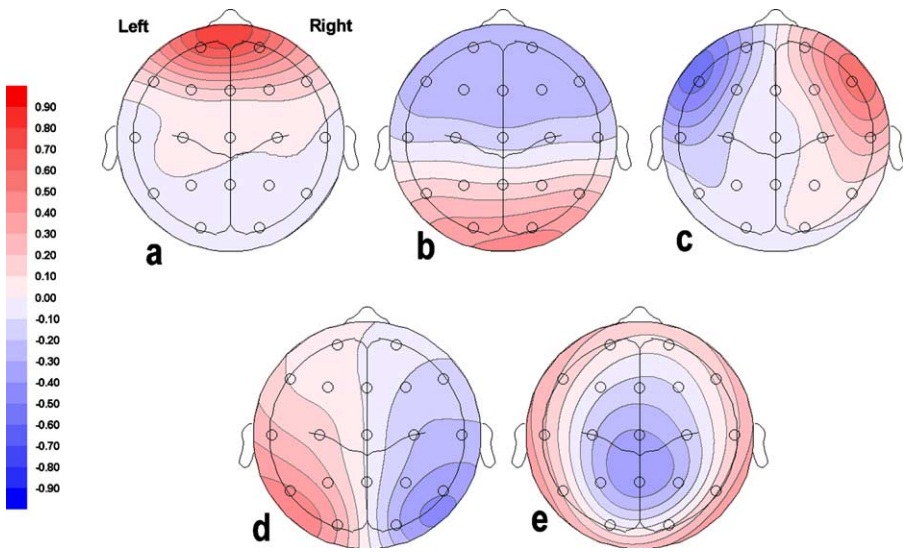

Fig. 4. Representations, as head maps, of the 5 spatial components common to 40 patients in whom the EEG was reported as showing 'nothing abnormal'. The maps allow identification of the source activities. (a) Vertical eye artefact; (b) in-phase alpha activity; (c) horizontal eye artefact; (d) out of phase alpha activity; and (e) further alpha activity.

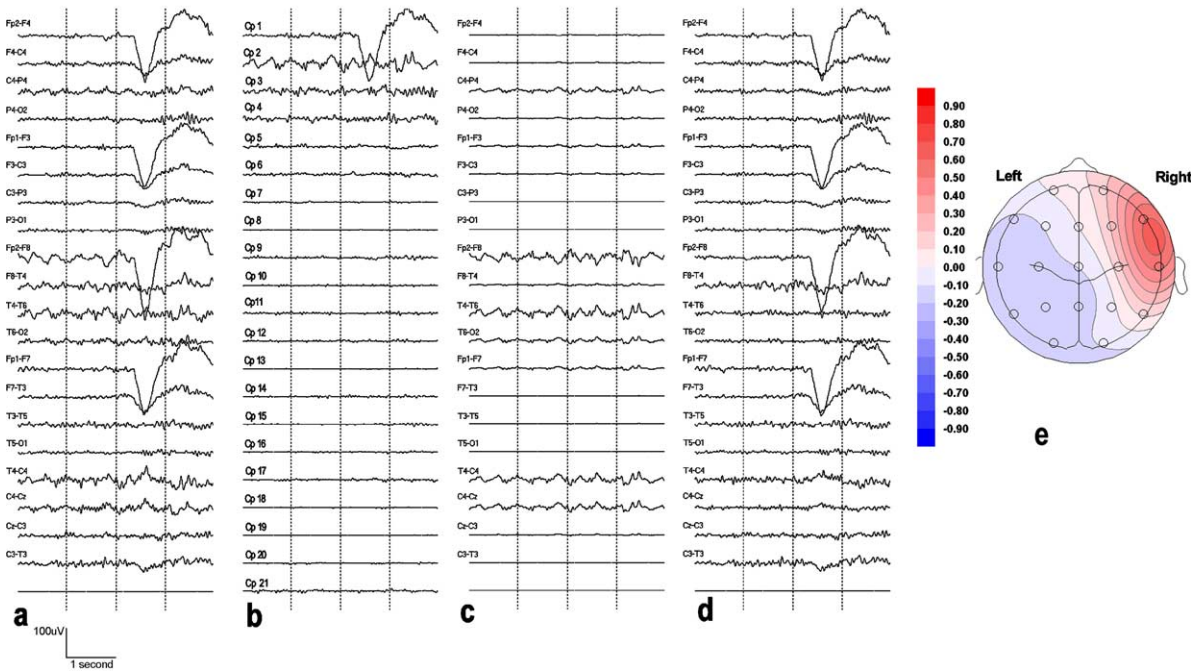

Fig. 5. A 68 year-old woman with a 3-month history of daily 'absences' lasting 1–2 min. (a) Four seconds of EEG from a record that shows right anterior quadrant focal delta activity. (b) The temporal components for the same sample of EEG; the delta activity is confined to component Cp2. (c) The contribution to the EEG of the abnormal component, Cp2. (d) Reconstruction of the EEG with the remaining 'normal' components, displaying the 'background' EEG and eye artefact. (e) Head map showing the distribution of spatial component Cp2.

represented by component Cp3 in Fig. 8b. Fig. 8c shows a reconstruction of the EEG using component Cp3 from Fig. 8b only, and hence shows the distribution of the theta activity across the bi-polar montage. Fig. 8e shows the head-map representing the spatial component corresponding to Cp3; it has a positive peak near the F7 electrode. Fig. 8d shows a reconstruction of the background EEG using all components, except component Cp3.

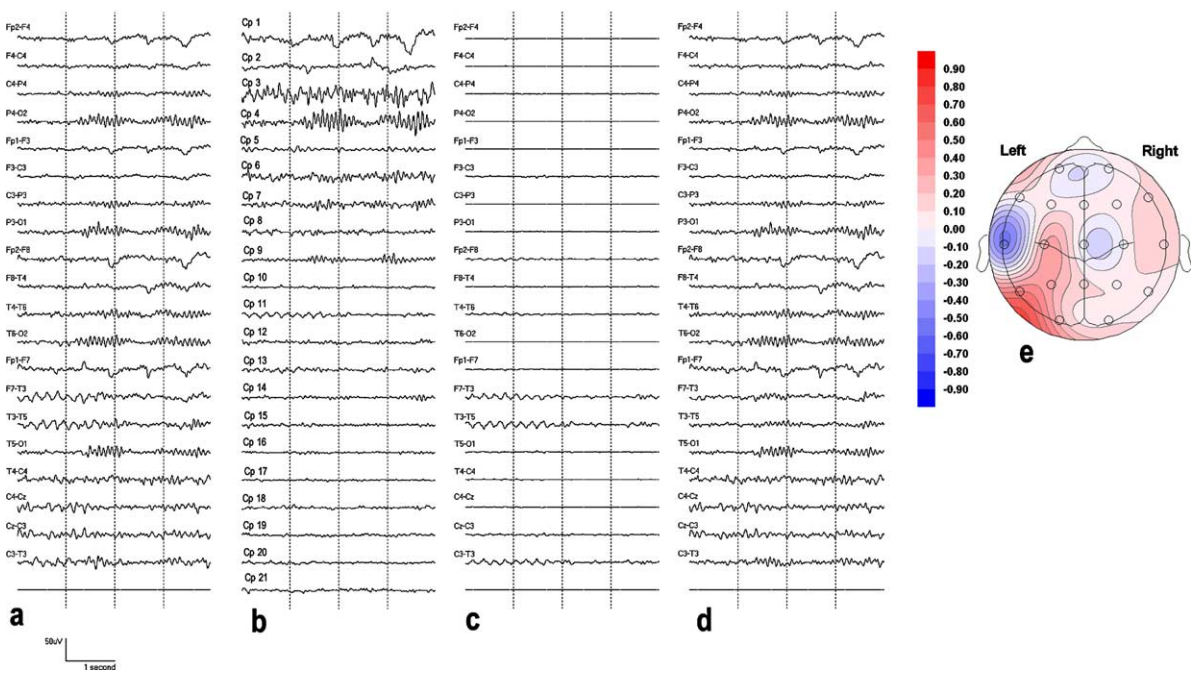

Fig. 6. A 24 year-old man with a congenital left hemiplegia due to a vascular incident, and a lifelong history of focal left sided motor seizures. (a) Four second section of an EEG showing focal rhythmic theta activity; (b) the temporal components for the same section of the EEG, components Cp11 and Cp13 contain the rhythmic theta activity; (c) the contribution to the EEG of the two 'abnormal' components; (d) reconstruction of the EEG using only the 'normal' components displaying the 'background' EEG and eye artefact; and (e) head map of spatial component Cp11.

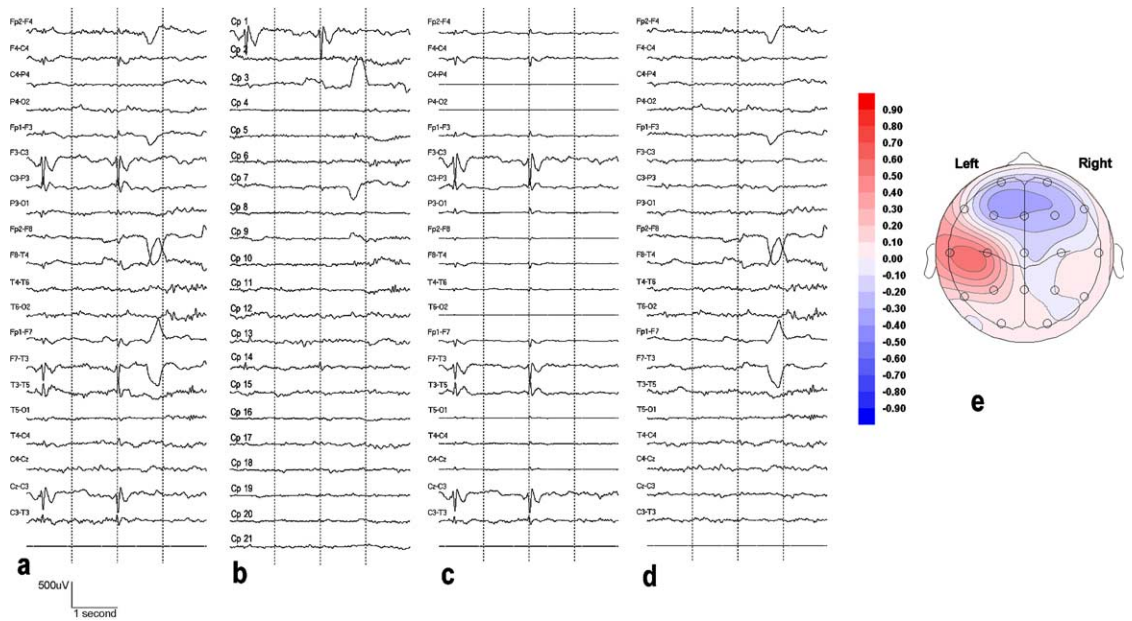

Fig. 7. A 29-month child with a 6-month history of 30 s episodes of left upper limb jerking on falling asleep. (a) Four seconds from an EEG that shows left mid-hemisphere focal spike and wave activity; (b) the temporal components: the first component Cp1 contains the majority of the spike and wave activity, with some residual activity on component Cp14; (c) the reconstruction of the EEG with the two spike and wave components Cp1 and Cp14; (d) a reconstruction of the EEG without the two 'abnormal' components: none of the spike and wave activity is visible in this reconstruction; and (e) head map showing the distribution of spatial component Cp1.

4. Discussion

A novel, clinically useful, spatio-temporal decomposition has been developed and validated for deriving the global spatial components of an EEG from the dominant components of short epochs of record; the resulting temporal components are unambiguously recognisable.

The method separates epochs dominated by different types of activity, by differentiating one cluster of spatial components, represented as points in N-dimensional space,

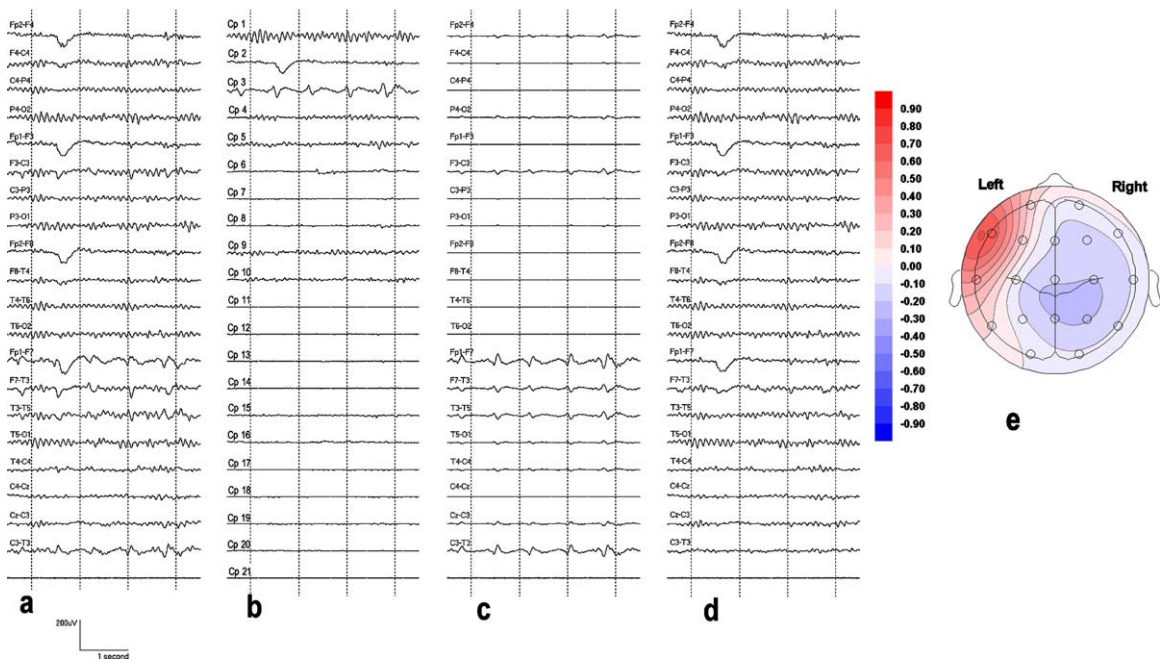

Fig. 8. A 60 year-old man with a 1 week history of focal seizure affecting the left upper and lower limb following a left hemiparesis. (a) Four seconds of EEG from a record that contains recurring left frontal sharp theta waves; (b) the temporal components from our method: the majority of the sharp theta activity appears on component Cp3; (c) the reconstruction of the EEG with the sharp theta component Cp3; (d) reconstruction of the EEG, without Cp3, the sharp theta component; and (e) head map showing the distribution of spatial component Cp3.

from another. It requires a record providing sufficient numbers of local estimates to form clusters, and in the case of a normal, awake record, 2 min duration, with an epoch length of a quarter second, sufficed. Activity could then be visualised, which would have been inappropriately decomposed by conventional PCA.

Any spatio-temporal method will not work when the number of sources of activity in the record is large relative to the number of channels (dimensions). This is different from a measurement such as Ω, the Wackermann complexity measure (Wackermann, 1999). In our method, activity from one source may appear only briefly, e.g. a single electrode artefact, but still count as a whole component required in the decomposition. With a measure like Ω, however, the artefact will only contribute a small fractional value to the final measure of complexity. We are exploring new ways of decomposing these less straightforward EEGs.

Observations made on 40 'normal' EEGs showed that there were two commonly occurring types of feature, eye related artefact and alpha rhythm. Most of these records contained two, or 3, significant alpha components. In most instances the main alpha spatial component showed a symmetrical posterior distribution. Further work will provide numerical values for normal ranges of the distribution of the alpha activity, and the ratio of the symmetric to asymmetrical components indicating different left/right amplitudes.

In most situations the eyes (and eyelids) move conjugately, so the analysis will only 'see' epochs that contain combined left and right eye artefact. In the eventuality the two sources mimic a single source. In most of the EEGs examined, two temporal components represented the majority of the eye-related artefact. These two temporal components represented the vertical and horizontal elements of the eye artefact; there was no separate component for the left eye and the right eye. Nevertheless, activity from the eyes and the brain are unlikely to be correlated so the analysis should be capable of separating them, and it may be possible, using this method, to perform eye artefact removal, potentially avoiding the problem of backward contamination of the estimates of the electro-oculogram (EOG) signal by the EEG, (Croft and Barry, 1998a,b, 2000) by finding simultaneous backward and forward regression coefficients between the EOG and EEG (Picton et al., 2000). In the example EEGs, however, there were no EOG electrodes. The inclusion of EOG electrodes would give a better estimate of the EOG signal, and improve its separation from other EEG activity and other artefact. The inclusion of EOG electrodes would also allow direct comparison with previously published eye artefact correction techniques, which invariably included EOG electrodes. Some of the 40 EEGs recorded in 'normal' people had more than two eye-related components and a more detailed study; with the addition of EOG electrodes might differentiate between eye and eyelid activity.

The choice of epoch length was arbitrary. The optimum epoch length is likely to depend upon the relative amounts of each activity present, and therefore, it might differ at different times within the record. The value of a 1/4 s, used to produce the results shown above, was a compromise but worked well. Also, the neighbourhood was defined as being within a distance of 0.25 to the cluster centre. The optimal value might be expected to change not only from record to record, but also from cluster to cluster within a single record. The fixed value of 0.25 used appears, however, to have been a satisfactory compromise.

Nevertheless, this novel method provides improved insight into the distribution of some forms of activity across the scalp; the head maps provide a simple, summary picture of the spatial distribution of activities seen in the EEG, and the corresponding spatial component vectors provide a numerical means for comparing the distributions of these components across records.

Acknowledgements

We gratefully thank Dr Patrick Berg, Konstanz University, for helpful comments and our colleagues Dr Marsha Morgan and Dr Sara Montagnese Centre for Hepatology, Royal Free Campus, Royal Free and University College Medical School, London, for additional comments. Head map display produced by the BPlot program from Berg P. ftp://klipsy/psychologie.uni-konstanz.de/Bplot/ or http://www.besa.de/.

Appendix A. The method

The whole EEG record is represented by the matrix X, where the columns represent a single sample at each of the N recording channels. The first step of the analysis splits the original EEG, X, into a number of smaller matrix representing a 1/4 s epoch.

$$X = [X_1 : X_2 : X_3 : \ldots X_1] \quad (1)$$

Each sub-matrix is multiplied by it's own transform to calculate the co-variance matrix for that epochs.

$$R_i = X_i * X_i^T \quad (2)$$

A PCA is performed on each co-variance matrix R_i separately to form a set of ortho-normal spatial components U_i, from which the temporal components V_i can be calculated. The spatial components are the columns of the matrix U_i, while the diagonal values in Σ_i describe the amount of the variance of the EEG they each account for. As each sub-matrix of the EEG, X_i, contain data from different times of the EEG, so the V_i and U_i matrixes will contain

different sets of temporal and spatial components.

$$R_i = U_i * \Sigma_i * U_i^T \quad (3)$$

$$V_i = \Sigma_i^{-1/2} * U_i^T * X_i \quad (4)$$

The first principal component from each epoch of EEG is used as an approximation to the dominant activity of that epoch. The first spatial component from each epoch of EEG X_i, that is the first column of each matrix U_i, is used as the coordinates of points in a N dimensional space, P_i. Where spatial components approximately describe the same dominant activity, the points will form a cluster. To find the main cluster, each point is assigned a density value, Q_i, based upon the distance between it (the point representing epoch i) and its neighbour's point (representing epoch j), and the amount of variance that neighbour accounts for in its epoch, v_j. A neighbour threshold distance of 0.25 was used.

$$d_{i,j} = (0.25 - \text{distance}(P_i, P_j))/0.25, \quad \text{when positive, else zero} \quad (5)$$

The distance factor varies from 1, where the points are on top of each other, to zero, where the distance between the points is 0.25 or greater.

$$v_i = \Sigma_i[1]/((\Sigma_i[1])^2 + (\Sigma_i[2])^2 + \cdots(\Sigma_i[N])^2)^{1/2} \quad (6)$$

The variance factor varies from 1, where there is only one type of activity in the epoch, and so all of the activity is described by the first principal component, to lower values where several principal components are required to fully describe the epoch's activity.

$$Q_i = \Sigma v_j d_{i,j} \quad (7)$$

The point P_i, nearest to the required cluster centre will be that with the largest density value, Q_i. To obtain a better estimate of the true cluster centre we calculated the average of the positions of those points within the neighbour threshold, weighted by their variance factors.

$$CC = \text{average } (v_j * P_j) \text{ for all j where distance } (P_i, P_j) <= 0.25 \quad (8)$$

As each new cluster centre, CC, is found it is normalised and added as the next column of a growing matrix of orthogonal spatial components O. From the pseudo inverse of the matrix O, O^P, a least squares best estimate of the corresponding temporal components is found, matrix M. The rows of M are not normalised, but are scaled according to their contribution to the EEG.

$$O^P = (O^T * O)^{-1} * O^T \quad (9)$$

$$M = O^P * X \quad (10)$$

From the O and X matrix, an estimate of the EEG accounted for by the found components can be obtained, X'.

$$X' = O * M \quad (11)$$

By subtracting this estimate, X', from the EEG, X, the result is that portion of the EEG not accounted for by the found components, X''.

$$X'' = X - X' \quad (12)$$

To find other components, this reduced EEG is fed back into Eq. (1). This loop continues until all N components have been found.

The spatial components found, O, are orthogonal and normalised.

$$O * O^T = I \quad (13)$$

The temporal components, corresponding to these spatial components, Q, are not orthogonal.

$$Q = O^T * X \quad (14)$$

$$Q * Q^T \neq I \quad (15)$$

The temporal components are made orthogonal by removing that proportion of each component which is not orthogonal to the other temporal components, and are renormalised, to obtain the final set of temporal components.

Once an ortho-normal set of temporal components is calculated, it is used with the original EEG data matrix, X, to obtain the spatial components d.

$$d = C^T * X \quad (16)$$

The spatial components in d are not normalised, so a set of factors is obtained in the diagonal elements of $E_{i,i}$, which scales the spatial components to form the matrix D.

$$E_{i,i} = (d_i * d_i^T) \quad (17)$$

$$D_i = d_i * \text{sqrt}(E_{i,i})^{-1} \quad (18)$$

The original EEG, X, is then reconstructed from the spatial components, the scaling factors, and the temporal components.

$$X = D * E^{1/2} * C \quad (19)$$

Appendix B

The K-means clustering algorithm

A K-means clustering algorithm attempts to find the position of the K cluster centres which best fit the data points, for a given value of K.

The method first allocates an arbitrary starting point for each of the K cluster centres. Each data point is than assigned to the cluster it is nearest to. The data points assigned to each cluster are weighted by there distance from the cluster centre, summed, and the sum is normalised to give the next position for that cluster centre. The distance each cluster centre moves is noted. This process of assigning data points to clusters, summing, normalising, and moving

the cluster centres continues until the distance moved by each cluster centre is below some lower threshold distance.

While this method finds the K cluster centres that best-fit the data points, the number of clusters found is chosen externally to the method, so some other method of determining the optimal number of clusters is required. In the case of our data, 5 very similar centres were found for values of K of 5, 6, 7 and 8, suggesting that the positions of these clusters were quite stable.

References

Croft RJ, Barry RJ. EOG correction: a new perspective. Electroenceph clin Neurophysiol 1998a;107:387–94.

Croft RJ, Barry RJ. EOG correction: a new aligned-artefact average solution. Electroenceph clin Neurophysiol 1998b;107:395–401.

Croft RJ, Barry RJ. Removal of ocular artefact from the EEG: a review. Neurophysiol Clin 2000;30:5–19.

Jung T-P, Makeig S, Westerfield M, Townsend J, Courchesne E, Sejnowski TJ. Removal of eye activity artefacts from visual event-related potentials in normal and clinical subjects. Clin Neurophysiol 2000; 111:1745–58.

Kaiser HF. The varimax criterion for analytic rotation in factor analysis. Psychometrika 1958;23:187–200.

Kobayashi K, James CJ, Nakahori T, Akiyama T, Gotman J. Isolation of epileptiform discharges from unaveraged EEG by independent component analysis. Clin Neurophysiol 1999;110:1755–63.

Kobayashi K, Merlet I, Gotman J. Separation of spikes from the background by independent component analysis with dipole modelling and comparison to intracranial recording. Clin Neurophysiol 2001;112: 405–13.

Koles ZJ. The quantitative extraction and topographic mapping of abnormal components in the clinical EEG. Electroenceph clin Neurophysiol 1991;79:440–7.

Koles ZJ. Trends in localization. Electroenceph clin Neurophysiol 1998; 106:127–37.

Lagerlund TD. EEG source localisation (model-dependent and model-independent methods). In: Niedermeyer E, da Silva F, editors. Electroencephalography. Basic principles, clinical applications, and related fields. Baltimore: Williams and Wilkins; 1998. p. 809–22.

Lamothe R, Stroink G. Orthogonal expansions: their applicability to signal extraction in electrophysiological mapping data. Med Biol Eng Comp 1991;29:522–8.

Pascual-Marqui RD, Gonzalez-Andino SL, Valdez-Sosa PA, Bisca-Lirio R. Current source density estimation and interpolation based on the spherical harmonic Fourier expansion. Intern J Neurosci 1988;43: 237–49.

Perrin F, Pernier J, Bertrand O, Echallier JF. Spherical splines for scalp potential and current source density mapping. Electroenceph clin Neurophysiol 1988;72:184–7.

Picton TW, van Roon P, Armilio ML, Berg P, Ille N, Scherg M. The correction of ocular artefacts: a topographic perspective. Clin Neurophysiol 2000;111:53–65.

Scherg M, von Cramon D. Two bilateral sources of the late AEP as identified by a spatio-temporal model. Electroenceph clin Neurophysiol 1985;62:32–44.

Vigario RN. Extraction of ocular artefacts from EEG using independent component analysis. Electroenceph clin Neurophysiol 1997;103: 395–404.

Wackermann J. Towards a quantitative characterisation of functional states of the brain: from non-linear methodology to the global linear description. Int J Psychophysiol 1999;34:65–80.

Wang Y, Berg P, Scherg M. Common spatial subspace decomposition applied to analysis of brain responses under multiple task conditions: a simulation study. Clin Neurophysiol 1999;110:604–14.